Modelling chemistry and transport in urban street canyons

Dai, Yuqing; Cai, Xiaoming; Zhong, Jian; MacKenzie, A. Robert

DOI:
10.1016/j.atmosenv.2021.118709

Modelling chemistry and transport in urban street canyons: Comparing offline multi-box models with large-eddy simulation

Yuqing Dai, Xiaoming Cai, Jian Zhong, A. Rob MacKenzie*
School of Geography, Earth & Environmental Sciences, University of Birmingham, Edgbaston, Birmingham B15 2TT, UK

*Corresponding author

AUTHOR EMAIL ADDRESSES:
Yuqing Dai: yxd598@bham.ac.uk
Jian Zhong: j.zhong.1@bham.ac.uk
Xiaoming Cai: x.cai@bham.ac.uk [retired]
A. Rob MacKenzie: a.r.mackenzie@bham.ac.uk

Corresponding author:
A. Rob MacKenzie: a.r.mackenzie@bham.ac.uk; telephone: +44 0121 414 6142.

Highlight

- NO_x-O_3-VOC chemical reactions are coupled with multi-box canyon models.
- The multi-box models reproduce flow characteristics in regular and deep canyons.
- Reactive species concentrations in street canyons are well captured in <1% of the run time of computational fluid dynamics.
- The impacts of segregation on reactive species can be investigated.

Abstract

Computational fluid dynamics models are resource-intensive, particularly when complex chemical schemes are implemented, and this computational expense limits their use in sensitivity analyses. We propose a flexible multi-box model that permits spatial disaggregation of sources and depositions to simulate the transportation and distribution of chemical species in street canyons with any aspect ratios for which a large eddy simulation (LES) of the flow exists. The spatial patterns of reactive species in the multi-box simulations are in good agreement with those from the LES, especially for the deep canyon from which air escapes more slowly. The overestimation of the LES simulation

worsens somewhat due to segregations when the chemistry of volatile organic compounds (VOCs) is included but the overall pattern is captured in a modelling framework. By reducing computational costs by several orders of magnitude, the multi-box model allows more sensitivity testing than the LES, and is an effective approach to investigate spatial pattern of fast non-linear chemistry or microphysics at the street scale.

Keywords: Air quality; Urban air pollution; Box models; Street canyon; Nitrogen dioxide; Ozone

1. Introduction

Street canyons typically combine to build up a semi-enclosed urban environment with high concentrations of anthropogenic pollutants trapped inside, leading to persistent higher exposure risk for pedestrians near the roadside (Ahmad et al., 2005; Oke, 1988; Vardoulakis et al., 2003). Canyons can be divided into three types in terms of the ratio of building height (H) to street width (W), namely aspect ratio (AR): wide canyons (AR < 0.3), regular canyons (AR ≈ 1), and deep canyons (AR > 1.3) (Vardoulakis et al., 2003). Oke (1988) classified the canyon flows into three isothermal regimes according to AR and L/W (L is the building length along the span-wise direction). These regimes include skimming flow (0.66 < AR < 1.57), wake interference flow (0.1 < AR < 0.66) and isolated roughness flow (AR < 0.1). Besides the isolated roughness flow, wake interference flow, and skimming flow, there is the fourth flow regimes, i.e., multi-vortex flow regime in deep street canyons. If Reynolds (Re) number independence is satisfied, there is only one-vortex when AR is 1 and 3, but two main vortexes appear when AR is 5 or more (Yang et al., 2020). However, in wind-tunnel-scale street canyons (H = 6 cm, Re~1.2×10^4), if Re number is not sufficiently large, there are two contra-rotative vortices when AR = 2 and three to five vertically aligned vortices when AR is 3-5 (Li et al., 2008). The main difference between these two groups is whether the requirement of Re-number independence is satisfied or not. Chew et al. (2018) proposed that the widely adopted criterion Re > 11,000 for ensuring Reynolds-number-independence (Re-independence) is not applicable for 2D street canyons as AR > 1.5. They discovered that only one primary vortex appeared when AR = 2 if Re > 8.7×10^4. Moreover, Yang et al. (2021) found that isothermal urban airflows for full-scale deep canyons can be independent of Re when Re exceeds 1×10^6 and 1×10^7 when AR is 3 and 5.

Because of much of the human exposure to outdoor air pollutants occurs at the pedestrian level in street canyons, understanding airflow characteristics and distributions of pollutants is of vital importance in evaluating the pollutant health risk and in making policy for targeted air pollution alleviation. The concentration of a passive scalar (PS, an idealised chemically inert substance that negligibly interferes with local fluid dynamics through effects such as buoyancy) can exhibit sharp gradients at the pedestrian level of the street canyons (Fellini et al., 2020; Lietzke and Vogt, 2013; Murena et al., 2009). Furthermore, the dispersion of atmospheric pollutants within the canyon is accompanied by complex non-linear chemical reactions, evolving on the timescale comparable to the canyon circulation and residence timescale. During the past two decades, studies have focused on the investigation of time-evolution and spatial variations of reactive species, for example, nitric oxide (NO), nitrogen dioxide (NO_2), and ozone (O_3) in street canyons, using coupled computational fluid dynamics (CFD) such as Reynolds-Averaged Navier-Stokes (RANS) and Large-Eddy Simulation (LES) models with different chemical schemes. Baker et al. (2004) integrated an LES model with a simple NO_x-O_3 cycle (two reactions in sunlight) to simulate the dispersion and spatial distribution of reactive species in a regular street canyon. The impacts of dynamics on the chemistry had been investigated by introducing the concept of the photo-stationary state defect (PSSD). Low PSSD values indicate equilibrium-like chemistry and were found at the centre of the primary vortex and on the windward corner at the street level. High PSSD values indicate rapidly-changing chemistry and were found at the location near NO_x sources, along the leeward facet (where pollutants were escaping the street canyon), and along the windward wall on the outer edge of the vortex (where fresh air was entrained into the canyon). Baik et al. (2007) adopted the renormalised k-ε RANS model coupled with the simple NO_x-O_3 photochemistry to simulate pollutant dispersion with the effects of street-bottom heating; Kwak and Baik (2012) further incorporated Volatile organic compounds (VOC) chemistry into the model and discussed the sensitivity of O_3 concentrations to NO_x and VOC emissions. Kim et al. (2012) examined reactive species in a regular canyon using RANS with a comprehensive tropospheric NO_x-O_3-VOC chemistry from GEOS-Chem. They found a substantial influence of different chemical schemes on O_3 levels and highlight the importance of more explicit chemistry simulation. However, Bright et al. (2013) found that VOCs could contribute additional but modest NO_2 and O_3 formation (about 12%) in the regular canyon, which is consistent with Garmory et al. (2009). Zhong et al. (2017) extended the LES model with the NO_x-O_3-VOC chemistry to simulate the spatial distribution of reactive species in an idealised deep urban street canyon. They revealed that volume-averaged NO_2 and the total oxidants (O_x) concentrations significantly increased due to VOCs-relating chemistry. Their works provided a better understanding of the combined effects of insufficient mixing and non-linear reactions in street canyons with a higher aspect ratio. Zhang et al. (2020) conducted RANS simulations with a simple NO_x-O_3 cycle in street canyons with AR = 1, 3 and 5, but their work neglected the effect of organic free radicals, which is likely important in determining the concentration of reactive species inside deep street canyons. Recently, Wu et al. (2021) developed a platform that integrated a CFD model (i.e., OpenFOAM) and a photochemical mechanism including VOCs for pollutant dispersion in the regular canyon. Although these CFD-based studies provide promising methods in order to simulate physical dispersion and chemical transformation of reactive species within canyons, modelling scenarios in reality are much more sophisticated in terms of, for example, emissions (Wu et al., 2021), wind conditions, roof shapes (Takano and Moonen, 2013), ground or wall heating (Cai, 2012), and the presence of green infrastructures such as trees with varying leaf area density (Abhijith et al., 2017; Gromke et al., 2008; Gromke and Ruck, 2007). The domain/model configurations need to be adjusted from case to case, and using a CFD model is, in general, very computationally expensive for the study of such a wide range of scenarios, especially when explicit VOC chemical reactions are included.

A more convenient and efficient way is adopting offline simulations, as is routinely employed at regional and global scales (e.g., Jacobson and Jacobson (2005); Kukkonen et al. (2012)). The zero-dimensional one-box model can easily adopt complex chemistry without intensive computational resources. It also exhibited satisfactory performance compared to the LES (Bright et al., 2013), despite relatively higher modelled NO, NO_2 and hydroxyl radical (OH) concentrations. Zhong et al. (2016) implemented a coupled two-box model with NO_x-O_3-VOC chemistry for simulating pollutants in a deep canyon. They highlight that the one-box treatment would miscalculate flow structure and pollutant gradients, and, hence, underestimate the exposure risk of pedestrians to NO_2 in the deep canyon. However, these simplified box models are still too coarse to evaluate air quality conditions at the pedestrian level. They would systematically neglect substantial concentration contrasts near the centre of the carriageway and cannot capture the horizontal distribution of pollutants, which is as important as vertical features in street canyons. The lack of available process-based methods makes it difficult to investigate systematically coupled chemistry-transport effects in street canyons.

In this study, a multi-box model with a flexible number of boxes and flexible chemical schemes has been developed for air pollution simulations in street canyons. The model design, mathematical formulation, and configurations for testing are described in Section 2. In Section 3, the modelling results of reactive species from the multi-box models with a reduced NO_x-O_3-VOC chemistry and a simple NO_x-O_3 cycle are evaluated against the published modelling data from the LES dynamical models at the box grid resolution, for idealised regular and deep street canyons. The time-evolution of concentrations, segregation effects due to overly fast chemistry in the multi-box case, and spatial variations inside canyons are discussed in detail. The conclusions and future perspective are summarised in Section 4. Although not the focus of the current paper, we note that aerosol microphysics introduces non-linear processes in street canyons in a similar way to chemistry (Gelbard and Seinfeld, 1980; Jacobson and Seinfeld, 2004; Jacobson et al., 1996; Zhong et al., 2020a, b; Zhong et al., 2018); the modelling framework described below could be extended to include detailed size-dependent aerosol microphysics in the future.

2. Methods

2.1. Description of models

2.1.1 The multi-box model

The principle of the multi-box model is to split the volume of street canyons into several boxes, where each box ideally reflects a resolved airflow arising from the aspect ratio or physical obstructions in street canyons (e.g., Fig. 1). In the two-dimensional framework, boxes inside the model are indexed based on their locations in Cartesian coordinates. Assuming the background wind above the roof level blows across the street canyon from left to right, starting from the bottom-left to the top-right, e.g., $Box_{[1,1]}$ represents the leeward corner of a canyon. Pollutant transfer between adjacent boxes is determined by the mean wind advection and by turbulent diffusion across the mesh interface. Vertical (denoted by capital "*G*") and horizontal (denoted by capital "*F*") mixing-ratio fluxes (ppb m s^{-1}) for pollutant, *q*, into $Box_{[k,i]}$ (i.e., "k" represents vertical index position, "i" represents horizontal index position) can be formulated as:

$$F_{e,[k,i]} = u_{e,[k,i]}\left(C_{q,[k,i-1]} - C_{q,[k,i]}\right) \quad (1)$$

$$F_{a,[k,i]} = \begin{cases} U_{a,[k,i]}C_{q,[k,i-1]}, U_{a,[k,i]} \geq 0 \\ U_{a,[k,i]}C_{q,[k,i]}, U_{a,[k,i]} < 0 \end{cases} \quad (2)$$

$$G_{e,[k,i]} = w_{e,[k,i]}\left(C_{q,[k-1,i]} - C_{q,[k,i]}\right) \tag{3}$$

$$G_{a,[k,i]} = \begin{cases} W_{a,[k,i]}C_{q,[k-1,i]}, W_{a,[k,i]} \geq 0 \\ W_{a,[k,i]}C_{q,[k,i]}, W_{a,[k,i]} < 0 \end{cases} \tag{4}$$

where $G_{a,[k,i]}$ (ppb m s^{-1}) and $F_{a,[k,i]}$ (ppb m s^{-1}) are mixing-ratio fractional fluxes due to advective transfer (i.e., flow resolved by the LES); $G_{e,[k,i]}$ (ppb m s^{-1}) and $F_{e,[k,i]}$ (ppb m s^{-1}) are mixing-ratio fluxes due to turbulent diffusion formulated by the Fick's law. $W_{a,[k+1,i]}$ (m s^{-1}) and $U_{a,[k,i+1]}$ (m s^{-1}) are the advective transfer velocities in the vertical and horizontal directions, respectively; and $w_{e,[k+1,i]}$ (m s^{-1}) and $u_{e,[k,i+1]}$ (m s^{-1}) are transfer velocities due to turbulent diffusion. By assuming all fluxes as vectors with positive values along the coordinate directions, the concentration in Box$_{[k,i]}$ can be calculated from the following equation:

$$\frac{dC_{q,[k,i]}}{dt} = E_{q,[k,i]} - \frac{G_{a,[k,i+1]} + G_{e,[k,i+1]}}{l_i} + \frac{G_{a,[k,i]} + G_{e,[k,i]}}{l_i} - \frac{F_{a,[k+1,i]} + F_{e,[k+1,i]}}{h_k} + \frac{F_{a,[k,i]} + F_{e,[k,i]}}{h_k} + \Delta S_{q,[k,i]} + \Delta V_{q,[k,i]} \tag{5}$$

where $C_{q,[k,i]}$ (ppb) is the mixing-ratio of the q^{th} species in Box$_{[k,i]}$, $E_{q,[k,i]}$ (ppb s^{-1}) is the emission rate of the q^{th} species into Box$_{[k,i]}$, h_k (m) and l_i (m) are the box height and box width respectively, $\Delta S_{q,[k,i]}$ (ppb s^{-1}) is the net production rate of the q^{th} species due to chemistry in Box$_{[k,i]}$, and $\Delta V_{q,[k,i]}$ (ppb s^{-1}) is the net deposition term of the q^{th} species in Box$_{[k,i]}$. Allowing computations with more species, and where the associated $\Delta S_{q,[k,i]}$ terms reflect more complicated non-linear chemistry, is one of the prime motivations for the development of the box model. By default, the boundary layer above the street canyon is assumed as one compartment, representing relatively steady background conditions over a long period (e.g., 1 hour). The 4th order Runge-Kutta method is adopted in the multi-box model to solve the ordinary differential equations (ODEs) numerically. To facilitate a systematic investigation, we use two dimensionless ratios to represent the size of grid boxes to the entire street canyon:

$$\alpha_k = \frac{h_k}{h_0} \tag{6}$$

$$\beta_i = \frac{l_i}{l_0} \tag{7}$$

where h_0 (m) and l_0 (m) are the canyon height and street width, respectively. Then the volume-averaged concentrations of q^{th} species ($C_{q,\text{m}\times\text{n-box}}$) for the entire canyon with m × n boxes is:

$$C_{q,\text{m}\times\text{n-box}} = \sum_{\text{k=1;i=1}}^{\text{k=m;i=n}} \alpha_\text{k} \beta_\text{i} C_{q,[\text{k,i}]} \quad (8)$$

If the volume is equal for all the boxes in street canyons, that is, i.e., $\alpha_1 = \alpha_2 = ... = \alpha_\text{k} = \frac{1}{\text{m}}$ and $\beta_1 = \beta_2 = ... = \beta_\text{i} = \frac{1}{\text{n}}$, then the equation (8) can be rewritten to:

$$C_{q,\text{m}\times\text{n-box}} = \frac{\sum_{\text{k=1;i=1}}^{\text{k=m;i=n}} C_{q,[\text{k,i}]}}{\text{m} \times \text{n}} \quad (9)$$

Additionally, a dimensionless factor $\gamma_{q,[\text{k,i}]}$ is adopted to account for the heterogeneous on-road emission of the q^{th} species:

$$\gamma_{q,[\text{k,i}]} = \frac{\alpha_\text{k} \beta_\text{i} E_{q,[\text{k,i}]}}{\sum_{\text{k=1;i=1}}^{\text{k=m;i=n}} \alpha_\text{k} \beta_\text{i} E_{q,[\text{k,i}]}} \quad (10)$$

Up to *n* continuous line sources could be added into the k^{th} (k = 1, 2, …, m) layer of the canyon, which is helpful for elevated road or rail sources and for biogenic emissions from street trees. $\gamma_{q,[\text{k,i}]} = 0$ or $\gamma_{q,[\text{k,i}]} = 1$ indicates that no emission or all vehicle emissions have been injected into $\text{Box}_{[\text{k,j}]}$.

In order to derive net chemical terms especially for short-lived reactive species such as hydroxyl radical (OH) and hydroperoxyl radical (HO_2), the ODEs of a chemical system for q^{th} species can be written as:

$$\frac{d}{dt} C_{q,[\text{k,i}]} = P_{q,[\text{k,i}]} - L_{q,[\text{k,i}]} C_{q,[\text{k,i}]} \quad (11)$$

where $P_{q,[\text{k,i}]}$ and $L_{q,[\text{k,i}]}$ are the chemical production and loss rates in the specific $\text{Box}_{[\text{k,i}]}$. If those chemical kinetics remain constant during a given timestep, Δt, equation (11) may be solved numerically with the quasi-steady-state approximation (QSSA):

$$C_{q,[\mathrm{k,i}],t_0+\Delta t} = \frac{P_{q,[\mathrm{k,i}],t_0}}{L_{q,[\mathrm{k,i}],t_0}} + \left(C_{q,[\mathrm{k,i}],t_0} - \frac{P_{q,[\mathrm{k,i}],t_0}}{L_{q,[\mathrm{k,i}],t_0}} \right) e^{-L_{q,[\mathrm{k,i}],t_0}\Delta t} \tag{12}$$

where t_0 represents the starting point of each time interval during simulations. The chemical lifetime of q^{th} species, $\tau_{q,[\mathrm{k,i}]}$, in the $\mathrm{Box}_{[\mathrm{k,i}]}$ is:

$$\tau_{q,[\mathrm{k,i}]} = \frac{1}{L_{q,[\mathrm{k,i}]}} \tag{13}$$

If $\tau_{q,[\mathrm{k,i}]} < 0.1\Delta t$, chemical reactions are extremely fast compared to Δt, which means the chemical-steady-state can be adopted:

$$C_{q,[\mathrm{k,i}],t_0+\Delta t} = \frac{P_{q,[\mathrm{k,i}],t_0}}{L_{q,[\mathrm{k,i}],t_0}} \tag{14}$$

If $\tau_{q,[\mathrm{k,i}]} > 100\Delta t$, chemical reactions take through much slower compared to Δt, and the forward Eulerian formula can be used:

$$C_{q,[\mathrm{k,i}],t_0+\Delta t} = C_{q,[\mathrm{k,i}],t_0} + \left(P_{q,[\mathrm{k,i}],t_0} - L_{q,[\mathrm{k,i}],t_0} C_{q,[\mathrm{k,i}],t_0} \right)\Delta t \tag{15}$$

If $0.1\Delta t < \tau_{q,[\mathrm{k,i}]} < 100\Delta t$, then the chemical timescale has a comparable magnitude with Δt, and equation (12) is employed for the calculation. However, solving equation (12) incurs substantial computational costs in practice. Alexandrov et al. (1997) proposed an alternative way for the optimisation of the QSSA algorithm, which rationally expands the exponential term based on the Taylor expansion in the second order:

$$e^{-L_{q,[\mathrm{k,i}],t_0}\Delta t} \approx \frac{1}{1 + L_{q,[\mathrm{k,i}],t_0}\Delta t + 0.5(L_{q,[\mathrm{k,i}],t_0}\Delta t)^2} \tag{16}$$

and equation (12) can be reformatted as:

$$C_{q,[\mathrm{k,i}],t_0+\Delta t} = \frac{C_{q,[\mathrm{k,i}],t_0} + \left(1 + 0.5 L_{q,[\mathrm{k,i}],t_0} \Delta t\right) P_{q,[\mathrm{k,i}],t_0} \Delta t}{1 + L_{q,[\mathrm{k,i}],t_0} \Delta t + 0.5 (L_{q,[\mathrm{k,i}],t_0} \Delta t)^2} \quad (17)$$

In the one- and multi-box models, reactive species have been divided into two categories in terms of their chemical lifetime. For the regular and deep canyons, an empirical timestep value of 0.03 s was used with equation (15) for numerical integration of long-lived species (e.g., NO, NO_2, O_3), and a value of 0.003 s with the equation (17) was used for short-lived species (e.g., HO, HO_2). They are the same as those used in the LES (Bright et al., 2013; Zhong et al., 2015) based on the timescale of the turbulent eddies, which also indicates that no species are fully in steady state in urban street canyon environment.

The multi-box model is written in R version 3.6.2 (R Core Team, 2019) and Fortran 90 (using the Intel Fortran (IVF) Compiler) in the origin version 1.0, including three modules: the main program, the dynamical submodule, and a chemical submodule. Modularisation allows the model to be easily modified or updated for various research purposes, e.g., to investigate the impact of different chemical mechanisms on air quality in street canyons or to investigate in-canyon particle microphysics (cf., Nikolova et al. (2016)).

Additionally, a typical one-box model is used as a reference in this study, and the mathematical expression is (Liu and Leung, 2008):

$$\frac{dC_{q,0}}{dt} = E_{q,0} - \frac{w_{t,0}}{h_0}\left(C_{q,0} - C_{q,b}\right) + \Delta S_{q,0} + \Delta V_{q,0} \quad (18)$$

where a subscript "0" indicates that signs have the same meaning as those in the multi-box model but for a whole space of the street canyon in volume. The parameter $w_{e,0}$ (m s^{-1}) represents the "exchange velocity" between the street canyon and boundary layer above the rooftop. A two-box model is also used only for simulations in the deep street canyon, the mathematical expressions are (Murena, 2012; Zhong et al., 2016):

$$\frac{dC_{q,\mathrm{L}}}{dt} = E_{q,\mathrm{L}} - \frac{w_{t,\mathrm{L}}}{h_\mathrm{L}}\left(C_{q,\mathrm{L}} - C_{q,\mathrm{U}}\right) + \Delta S_{q,\mathrm{L}} + \Delta V_{q,\mathrm{L}} \quad (19)$$

$$\frac{dC_{q,\mathrm{U}}}{dt} = \frac{w_{t,\mathrm{L}}}{h_{\mathrm{U}}}\left(C_{q,\mathrm{L}} - C_{q,\mathrm{U}}\right) - \frac{w_{t,\mathrm{U}}}{h_{\mathrm{U}}}\left(C_{q,\mathrm{U}} - C_{q,b}\right) + \Delta S_{q,\mathrm{U}} + \Delta V_{q,\mathrm{U}} \qquad (20)$$

where subscripts “L” and “U” indicate that signs have the same meaning as aforementioned but for the lower and upper compartments (i.e., including 16 boxes in the red box to solve the main vortexes) of the deep street canyon in volume, respectively. $w_{e,\mathrm{L}}$ (m s^{-1}) represents the “exchange velocity” between two in-canyon compartments, and $w_{e,\mathrm{U}}$ (m s^{-1}) represents the “exchange velocity” between the upper compartment and the overlying background.

2.1.2 Large-eddy simulation

The LES results of reactive species were taken from Bright et al. (2013) for an idealised regular canyon, and from Zhong et al. (2017) for a deep canyon. Their studies applied OpenFoam v2.1.1 (Jasak et al., 2007) to resolve turbulence at large spatial and temporal scales and to simulate incompressible airflow with a high Reynolds number (Re $\sim 1\times10^{6}$) in street canyons under the neutral atmosphere. The unresolved sub-grid scales (SGS) processes were treated using the one-equation SGS turbulence model, and the logarithmic law of the rough-wall (Schlichting and Gersten, 2016) was used for the near-wall treatment. Symmetry boundary conditions were used for the domain overlying the canyon, and cyclic boundary conditions were employed in x- and y-directions. A constant pressure gradient in the upper background was assumed to produce a flow perpendicular to the canyon axis. The simulations of the LES were conducted with only dynamics for about 5 h in order to obtain a dynamical-steady flow field, which was further adopted as the initial turbulence condition.

For the regular canyon, the resolved turbulent kinetic energy (TKE) has been evaluated against wind-tunnel experiments (Cui et al., 2004) and the scalar has been validated by Cai et al. (2008); for the deep canyon, the flow field agreed well with water-channel (Li et al., 2008) and wind tunnel (Kovar-Panskus et al., 2002) experiments. The deposition of air pollutants is not considered in the LES modelling. The method for integrating VOC chemistry in the LES modelling is similar to that of the multi-box simulations described above and has been detailed in Zhong et al. (2017). The methods for initialising and processing the LES (e.g., emission, time step) are also adopted directly for the multi-box model and are described in the following section.

2.2. Model configurations

2.2.1 Street canyon geometry

The LES domains adopted for regular (AR = 1) and deep (AR = 2) canyons were presented in Fig. 1(a) and Fig. 1(b), respectively. In the LES, mesh resolutions were 0.3 m, 1.0 m and 0.3 m in the x, y, z directions, respectively, inside street canyons. That is, there are respectively 3,600 and 7,200 cells inside regular and deep canyons in the LES simulations. For the layer above the canyon in the LES simulation, Δz gradually increased by a factor of 1.15 from the rooftop to the domain top (z_0 = 18-90 m and z_0 = 36-112 m for regular and deep canyons). Fig. 1(c) and Fig. 1(d) are the respective counterparts in multi-box models for the cross-section canyons. The building height and street width are 18 m ($h_0 = l_0$) for the regular street canyon, and are 36 and 18 m ($h_0 = 2l_0$) for the deep street canyon. The red frame in Fig. 1(d) presents a two-box model with $h_\mathrm{L} = h_\mathrm{U}$ = 18 m. One primary clockwise vortex forms in the simulations of the regular canyon as the background skimming wind perpendicularly blows along the x-direction across the canyon axis; however, in the deep street canyon, a clockwise vortex in the upper compartment and a weak counter-clockwise vortex in the lower compartment are formed. In the multi-box model, the in-canyon volumes have been divided into identical 16 and 32 boxes for the regular and deep canyons, respectively (namely the 16- and 32-box models). This implies that each grid has a volume of 4.5 m × 1 m × 4.5 m = 20.25 m^3.

2.2.2 Dynamical parameters for air mass exchange

The exchange velocity ($w_{e,0}$) for the one-box model, and the advective and turbulent velocities for the multi-box model, are of the utmost importance in determining the intensity of in-canyon mixing, and transport and rates of escape of atmospheric pollutants to the overlying background. The values of $w_{e,0}$ = 0.022 m s^{-1} and $w_{e,0}$ = 0.012 m s^{-1} are respectively adopted for the cross-section 18 m × 18 m regular and 18 m × 36 m deep canyons (as in Fig. 1) in the one-box model, corresponding to a reference wind velocity of 2 m s^{-1} in the above rooftop layer under the neutral conditions (Cai, 2012a; Zhong et al., 2017). The values of $w_{e,\mathrm{L}}$ = 0.0229 m s^{-1} and $w_{e,\mathrm{U}}$ = 0.0156 m s^{-1} are used for the two-box simulation in the deep canyon, respectively.

In order to quantify the transport due to advection ($W_{a,[\mathrm{k,i}]}$ and $U_{a,[\mathrm{k,i}]}$, denote "advective velocities" in this study) and mixing due to turbulence ($w_{e,[\mathrm{k,i}]}$ and $u_{e,[\mathrm{k,i}]}$, denote "turbulent velocities") in the multi-box model, firstly vertical mixing-ratio fluxes including advective fluxes and turbulent fluxes of PS at the interface of boxes were extracted from the LES modelling results, and the averaged values over a period of the last 60 minutes were used for calculations. The total horizontal fluxes were then derived based on the flux balance of each grid on the Eulerian coordinates under an assumed equilibrium state over the period. These LES-derived fluxes describe the transmission of PS between any two adjacent boxes in street canyons. However, the velocities from the LES simulations (representing "real" wind conditions) cannot be used directly, because they need to be adjusted to calculate the mass transfer between coarser grids. Therefore, pollutant advective velocities ($U_{a,[\mathrm{k,i}]}$ and $W_{a,[\mathrm{k,i}]}$) are obtained using the vertical advective fluxes ($F_{a,[\mathrm{k,i}]}$ and $G_{a,[\mathrm{k,i}]}$) and the grid concentrations (i.e., an volume-averaged value at the grid resolution of the multi-box model) following Equation (2) and (4), and vertical mixing-ratio turbulent velocities ($w_{e,[\mathrm{k,i}]}$ and $u_{e,[\mathrm{k,i}]}$) are obtained using vertical turbulent fluxes ($F_{e,[\mathrm{k,i}]}$ and $G_{e,[\mathrm{k,i}]}$) and concentration gradients based on Equation (1) and (3). In this way, the mass fluxes of the multi-box and LES models are consistent at the same box interface under the equilibrium state. It is noted that the derivation for horizontal fluxes may have uncertainties because emissions from a single line source are simply assumed to be injected into one grid in the multi-box model, whereas a Gaussian distribution over the carriageway was assumed in the LES model. A coarser grid resolution can reduce this type of error. Therefore, in this study, the 16- and 32-box models are used to evaluate reactive species in regular and deep urban street canyons, and the details of advective and turbulent velocities are presented in the support information (Table S1 and Table S2). Model performance under higher horizontal resolutions is left to be evaluated in future work.

Due to the very similar magnitude of advective fluxes entering and escaping the street canyon in the neutral atmosphere (Salizzoni et al., 2009), the escaping canyon fluxes due to vertical advection are rotated into the horizontal direction, and thus the multi-box model considers only turbulent terms at the rooftop. Turbulent velocities as described above could be negative (although usually of small magnitude in such cases), indicating counter-gradient turbulent diffusion under the box-model framework (Figs. 1c and 1d). This may cause the model to crash during a box model timestep if concentrations become negative. In order to address this issue, a minimum positive value of 1.0×10^{-4} m s^{-1} is applied to the turbulent velocity, implying a very small turbulent flux compared to the advective flux for the interface under such conditions.

2.2.3 Emissions and chemical mechanism

Traffic-related pollutants were emitted by two consecutive line-sources at 1 m height and at 2.5 m to the left and right of the street centre axis for the LES models. Therefore the emissions were evenly injected into $Box_{[1,2]}$ and $Box_{[1,3]}$ at the street level for the multi-box models ($\gamma_2 = \gamma_3 = 0.5$). The emission rates of NO, NO_2, carbon monoxide (CO), ethene (C_2H_4), propene (C_3H_6), formaldehyde (HCHO) and acetaldehyde (CH_3CHO) were calculated based on the UK Road Vehicle Emission Factors (Boulter et al., 2009), which were 558, 62, 1356, 56, 24, 32 and 15 g km^{-1} hr^{-1}, representing a typical weekday traffic scenario of 1500 vehicles per hour with an average speed of 30 miles per hour (mph), which equate to 900, 100, 3593, 347, 150, 96 and 98 ppb s^{-1} for the LES cell; to 4.0, 0.44, 16, 1.55, 0.67, 0.88 and 0.42 ppb s^{-1} for the 16- (and 32-) box grid; and to 0.252, 0.028, 1.0, 0.097, 0.042, 0.055 and 0.026 ppb s^{-1} for the one-box grid in the regular canyon and for the two-box grid in the deep canyon. Moreover, PS that only undergoes physical processes was injected at the same rate with NO_x (= NO + NO_2) to investigate the sole effect of canyon dynamics on the model performance.

The Reduced Chemical Scheme (RCS) was developed by Bright et al. (2013), based on the Common Representative Intermediates mechanism version CRI *v2-R5* (Watson et al., 2008). The RCS retains the compounds that have important effects on core chemical intermediates in urban street canyons and includes 51 gas-phase species and 136 chemical reactions. The chemical kinetics are calculated at 20°C under a standard atmosphere pressure (e.g., photodegradation rate of 9.20×10^{-3} s^{-1} for NO_2), and they are adopted for simulating the daytime chemistry in the present study. The comparison between RCS and the benchmark Master Chemical Mechanism (12691 chemical reactions of 4351 species for MCM*v*3.0) (Saunders et al., 2003) showed that the maximum differences were 3%, 13%, 16%, and 12% for NO, NO_2, O_3 and OH during a four-hour simulation, which was comparable to, or smaller than, the errors from emissions and detection techniques (Boulter et al., 2009; Heard and Pilling, 2003). The total computation time of the multi-box model with RCS is about 6 minutes, which is higher than that of the one-box (~1 s) and two-box models (~8 s), but is significantly faster compared to those of the LES (around 10 days) (Zhong et al., 2017).

2.2.4 Model initialisation and output post-processing

The initial concentrations of the multi-box model are consistent with those in LES conditions for two types of canyons, which were taken from the field study of the Tropospheric Organic Chemistry

(TORCH) experiment (Lee et al., 2006). These observations represent a typical atmospheric condition in rural London, UK, during the summer of 2003. The models have been operated for 30 min "spin-up" period without any emission in order to initialise the chemical intermediates, then traffic emissions are switched on and concentrations of all species at t = 30 min are used as the cyclic "fixed" background conditions for a next 210 min modelling duration (i.e., t = 30-240 min) in a time step of 0.03 s. The solar radiation intensity remains constant during the model operation. "*zero background*" for PS is assumed during the LES and box operations.

The concentrations from box models were stored in an interval time step of 1 min for time-evolution analysis. The final hour of the modelling results (i.e., t = 180-240 min) was extracted for the calculation. Details about LES outputs pre-processing can be found in Bright et al. (2013) (for the regular canyon) and Zhong et al. (2015) (for the deep canyon), respectively. Subsequently, the modelling results of LES were averaged equivalent to the coarse resolution of box models for the purpose of evaluating the spatial distributions of air pollutants with the multi-box models. In order to investigate the impacts of incomplete mixing on the sub-grid scale variability due to chemistry, a widely-used dimensionless parameter *intensity of segregation* (Krol et al., 2000) is adopted in this study:

$$I_{\mathrm{S}(q_1+q_2)} = \frac{\left\langle q_1^* q_2^* \right\rangle}{\left\langle q_1 \right\rangle \left\langle q_2 \right\rangle} \qquad (21)$$

where $I_{\mathrm{S}(q_1+q_2)}$ represents the intensity of segregation between chemical species q_1 and q_2, angle brackets refer to the volume-averaged conservation quality, defined by Equation (8) for the multi-box model, $<q_1^* q_2^*>$ represents the volume-averaged covariance between q_1 and q_2, and an asterisk means the deviation from the averaged value. So, for a general case, we have $\left\langle q_1 \right\rangle = \sum \alpha_{\mathrm{k}} \beta_{\mathrm{i}} C_{q_1,[\mathrm{k,i}]}$, $\left\langle q_2 \right\rangle = \sum \alpha_{\mathrm{k}} \beta_{\mathrm{i}} C_{q_2,[\mathrm{k,i}]}$, $q^*_{1,[\mathrm{k.i}]} = C_{q_1,[\mathrm{k,i}]} - \left\langle q_1 \right\rangle$, $q^*_{2,[\mathrm{k,i}]} = C_{q_2,[\mathrm{k,i}]} - \left\langle q_2 \right\rangle$, and $\left\langle q_1^* q_2^* \right\rangle = \frac{1}{16} \sum q^*_{1,[\mathrm{k,i}]} q^*_{2,[\mathrm{k,i}]}$. The volume-averaged second-order reaction rate ($<k_{(q_1+q_2)}>$) can be written as:

$$\left\langle k_{(q_1+q_2)} \right\rangle = k_{(q_1+q_2)} \left(1 + I_{\mathrm{S}(q_1+q_2)}\right) \qquad (22)$$

where $k_{(q_1+q_2)}$ is the original reaction rate in the sufficiently well-mixed one-box model. Therefore, $I_{S(q_1+q_2)}$ can also be thought of as quantifying the deviation from chemical equilibrium due to the spatial segregation associated with atmospheric dynamics. For any species in the one-box model, $I_{S(q_1+q_2)}$ equals to zero because there is no spatial segregation inside the box. A positive $I_{S(q_1+q_2)}$ indicates that $<k_{(q_1+q_2)}>$ in the 16-box model is larger than $k_{(q_1+q_2)}$ in the one-box model because of the segregation effect. When $q_1 = q_2$, $I_{S(q_1+q_2)}$ represents the spatial variability of any specific pollutant in respect to its canyon volume-averaged concentration.

3. Results and discussion

3.1. Temporal evolution and the intensity of segregation within the canyon

Fig. 2 shows temporal evolution of the volume-averaged pollutant mixing-ratios of the LES, and multi- and one-box models under the same raw emissions, meteorological conditions, and RCS chemistry as the LES model, in idealised regular (a, b) and deep (c, d) street canyons, respectively. Modelling results of the two-box model are available only for the deep canyon. The LES-RCS data for the regular and deep canyons are from Bright et al. (2013) and Zhong et al. (2017), respectively. The box models produce less temporal variability; reactive species slowly move toward a chemical-transport equilibrium. The O_3 concentrations drop sharply after zero-emission "spin-up" period due to NO and O_3 titration, accelerating the formation of NO_2 in street canyons. The OH and HO_2 concentrations rapidly relax to equilibrium when traffic emissions are switched on, the maintenance of a steady-state HO_2 by oxidation of VOCs contributes to an additional NO_2 fraction. The chemical species in the regular canyon achieve a transport-chemistry balance more quickly (i.e., about 90 min for NO and NO_2) than in the deep canyon (e.g., around two hours for NO and NO_2) in both one- and multi-box models, and the LES, because of more effective ventilation for canyons with a lower AR. The concentrations of selected species at the equilibrium state over the final hour of model operation are discussed below for a better understanding of the coupled dynamical and chemical processes in street canyons.

Table 1 illustrates the time-averaged mixing-ratios of PS, NO, NO_2, O_3, OH, HO_2, NO_x (= NO + NO_2), O_x (= NO_2 + O_3) and NO_2/NO ratios from the models coupled with the RCS chemistry during the final simulation period ($180 \leq t \leq 240$ min) in the regular and deep street canyons, respectively.

For the regular canyon, LES outputs are slightly different from those in Bright et al. (2013), because of the dynamics-driven variability in concentrations and the difference in averaging times (i.e., $180 \leq t \leq 240$ min in the current study vs. $150 \leq t \leq 210$ min). The modelled mean PS concentrations of box models are in good agreement with those of the LES-based models (differences within ±0.5%). The spatially-averaged NO concentrations over the canyon are underestimated up to 4% by the box models, while levels of other species are all overestimated to different extents, in particular with OH levels (overestimated up to around 38%). The overestimations of O_3 are about 5.7% and 2.8% by the one- and 16-box models compared to more accurate LES modelling results.

Previous modelling results (Bright et al., 2013) showed that the NO_x modelled by the zero-dimensional one-box model were about 8 ppb (3.3%) higher than by the LES, O_3 concentrations were underestimated by 6%, and NO was overestimated by around 1%. One explanation for the difference between the results of the, present study and the previous study is that the value of $w_{e,0}$ adopted for representing the canyon ventilation is ~5% higher in this study (i.e., $w_{e,0} = 0.22$) compared to their work (i.e., $w_{e,0} = 0.21$), resulting in a higher abundance of O_3 in the street canyon due to inward transport in from the background. The NO and NO_2 concentrations would be changed accordingly. It should be noted that NO_x increases by about 1.6% in the box models, which means NO_x loss processes (e.g., production of nitric acid and organic nitrates) are more effective in the LES model. The O_x levels are respectively 9.0% and 11.1% higher in the 16- and one-box models because the efficient mixing of background O_3 and in-canyon NO produces more NO_2 than under less efficient mixing conditions, which is further discussed in the following section.

For the deep canyon, it is noted that the coarse resolution leads to a systematic underestimation of about 3.0% in PS by the one-box model and of about 2% by the two-box model (Table 1); additionally, Table 2 presents the mixing-ratio of pollutants from the LES, 32-box and two-box models in the upper and lower compartments of the deep canyon, respectively. The 32-box model performs better than the two-box model in simulating PS in both compartments. This may be attributed to the definition of the exchange velocity (e.g., $w_{e,0}$, which is calculated based on the gradient between the whole canyon-averaged and the ambient concentrations) and other dynamical parameters. For example, the exchange velocities for the two-box and multi-box models are calculated based on the gradient between the concentrations in the rooftop boxes and the overlying background. This more local concentration gradient provides a better description for the flux balance in the multi-box model and thus, better modelling results (i.e., closer to the LES outputs).

The difference in the flux-balanced exchange velocities may also have important impacts on the chemistry in the canyon. The multi-box models include horizontal transport that can compensate errors in modelling the canyon-averaged concentration, as less PS levels (around 1.5%) are underestimated by the 32-box model. The box models overestimate reactive species except for NO compared to the LES, which is consistent with the tendencies in the regular canyon. The absolute errors between the LES and box models are larger for NO, NO_2 and O_3 but are smaller for OH and HO_2 in the deep canyon, partly due to poor ventilation. Moreover, different chemical regimes may exist in the canyon in terms of multi-vortices formed in the canyon, generating a complex outcome for the whole-canyon averages. O_x is overestimated, as in the regular canyon, but NO_x is underestimated partly because of the advective and turbulent velocities used in the model. The concentration differences show a consistent pattern going from the complete-mixing (i.e., one-box resolution) to resolved transport-and-mixing (i.e., LES resolution) conditions for most reactive pollutants. That is, the multi-box model in general presents closer-to-LES results than the one-box model. For example, instant mixing in street canyons accelerates more NO conversion to NO_2. Hence, NO_2 is overestimated around 13% by the one-box model but 10% by the 16-box model in the regular canyon; and it is overestimated about 15% by the one-box model, 13.6% by the two-box model, but 8.6% by the 32-box model in the deep canyon (Table 1 and 2). The NO_2/NO ratios gradually reduce from 0.53 to 0.45, and from 0.63 to 0.47 in the regular and deep street canyons from the one-grid approximation to the highest resolution, respectively. For the modelled concentrations of HO_x (= OH + HO_2), the results of all the box models are very close to each other. The rationale behind this similarity is discussed below using the intensity of segregation.

Table 3 compares the percentage intensities of segregation between any two selected chemical species from the LES and multi-box models in regular and deep street canyons. It shows that the most spatially variable air pollutant in the canyon is NO (i.e., indicated by $I_{S(NO+NO)}$) and the least spatially variable pollutant is OH (i.e., indicated by $I_{S(OH+OH)}$) in general. Not surprisingly almost all intensities of segregation in the deep street canyon are considerably higher (e.g., 26% for $I_{S(NO+NO)}$) than those in the regular canyon (e.g., 3% for $I_{S(NO+NO)}$), which are supported by Zhong et al. (2017). It indicates that NO concentrations become more heterogeneous due to the perturbed in-canyon vortexes, but OH is less affected in terms of their abundance and lifetime in street canyons. It is also found that within both types of canyons the values of $I_{S(q_1+q_2)}$ in the multi-box models mostly have a same sign with those in the LES, which is positive for "emitted-inside-canyon" species (i.e., NO, NO_2) and is negative for "entrained-from-background" and "formed in situ" species (i.e., O_3, OH, HO_2), indicating similar chemical behaviours (e.g., generation or depletion) of these species in the LES and multi-scale models.

For atmospheric pollutants that directly react with each other, the intensities of segregation of the multi-box models have a trend toward "zero" compared with the LES. For example, NO and O_3 titration rates are slower by 2.79% and 10.02% in regular and deep canyons under the "true" condition, but slower by only 1.34% and 9.35% respectively under the "multi-box" approximation at the current resolution. That is, the performance of multi-box model is in between the LES (i.e., close to the "true" flow, insufficient mixing with hundreds of thousands of boxes) and the one-box model (i.e., instant and homogeneous mixing with no segregation). On the contrary, the reactions of O_3 and HO_2 producing OH have been accelerated by 1.74% and 2.36% in the LES, but only by 0.42% and 1.56% in the multi-box models.

3.2. The spatial variation of pollutants in street canyons

Fig. 3 illustrates vertical profiles ($0 < z/l_0 < 0.25$, $0.25 < z/l_0 < 0.5$, $0.5 < z/l_0 < 0.75$, $0.75 < z/l_0 < 1.0$) of time-averaged PS, NO, NO_2, O_3, OH and HO_2 in the regular canyon (black lines), along with the leeward (blue lines) and windward walls (red lines) in order to further ascertain the performance of the multi-box model. In order to compare the model performance of the LES and multi-box model at the same grid resolution, the quantities of the LES were averaged over the entire street width ($-0.5 < x/l_0 < 0.5$) and the nearest box grid resolution adjacent to the canyon walls (i.e., $-0.5 < x/l_0 < -0.25$ for the leeward, $0.25 < x/l_0 < 0.5$ for the windward), respectively. The distributions of chemical species from the 16- and 32-box models are presented in the support information. Over the final hour of the simulation, it is clear that the vertical distributions of PS from the 16-box model are in good agreement (within 5 ppb) with those from the LES, with higher concentrations elevated on the leeward side of the street corner (305.0 ppb) and considerably lower concentrations on the windward side (172.2 ppb) due to the in-canyon air circulation. The agreement for PS indicates that the multi-box model with LES-driven dynamics captured the major flow pattern well (i.e., a primary vortex) within the regular street canyon.

The agreement for PS also implies that the discrepancies in the abundance of reactive species between the multi-box and the LES models are mainly attributed to NO_x-O_3-VOC chemical reactions, though their vertical and horizontal features are also well-reproduced by the multi-box model. NO concentrations are well-simulated in $Box_{[1,4]}$ (difference within 1 ppb) but are slightly underestimated at other grid points, especially for the leeward side (difference around 8 ppb, ~3%). Due to less segregation for the 16-box model, there is a more effective O_3 titration in the canyon, which depletes more NO turning to NO_2, thus causing an underestimation of NO and an overestimation of NO_2 contents in the 16-box model. Errors in NO_2 concentrations become smaller on the windward side but become larger on the leeward side from the street level to the canyon rooftop. The maximum overestimation of NO_2 is 15.6 ppb (19.1%) at $0 < z/l_0 < 0.25$ of the leeward side ($Box_{[1,1]}$) and 9.9 ppb (12.6%) at $0.5 < z/l_0 < 0.75$ of the windward side ($Box_{[3,4]}$). The O_3 concentrations are underestimated on the windward side with the maximum box-minus-LES value of 2.2 ppb (24.3%) at $0 < z/l_0 < 0.25$ ($Box_{[1,1]}$) due to effective titration with recirculated NO under the sufficient mixing condition. However, there is an clear overestimation in O_3 contents on the leeward side with the maximum difference of -3.6 ppb (19.1%) at $0.75 < z/l_0 < 1.0$ ($Box_{[1,4]}$). The explanation could be that more O_3 accumulated on the leeward side because of the rapid photodegradation of overproduced NO_2 due to segregation effects on the windward side. Moreover, higher O_x levels in the 16-box model may be attributed to overestimated HO_x concentrations (about 0.03 ppt for OH, 0.07 ppt for HO_2) in the street canyon.

The Damköhler number (Da) is a widely used ratio of the chemical reaction rate to the diffusion rate (or, equivalently, the ratio of diffusion timescale to reaction timescale) for determining the importance of segregation effects on reactive species (Driscoll et al., 1992). If Da << 1, the dynamics achieve "equilibrium" much faster than the reaction, leading to minimal segregation effects for the pollutant; if Da >>1, the reaction may be considered to reach equilibrium instantaneously compared to the relatively slower diffusion rates. That is, dynamics for the pollutants with substantial segregation effects must be considered in a coupled manner (Garmory et al., 2006). Zhong et al. (2017) reported the Da numbers of NO, NO_2, O_3, OH and HO_2 in the street canyon, which were 3.4, 5.8, 69, 1.44×10^5 and 4.44×10^4, respectively. The chemical reaction rates of HO_x are much quicker than the diffusion rates across the model grid (Da >> 1). This explains that HO_2 is 0.02 ppt higher on the windward side compared to the leeward side, and vertical distributions of OH and HO_2 from the 16-box model are not significant compared to the outputs of the LES.

Fig. 4 shows the vertical distributions of selected species in the deep canyon and along with the leeward and windward facets. The PS concentrations of the 32-box model are well-matched to those of the LES model in both vertical and horizontal directions, with an underestimation of around 10 ppb (2.4%) on the leeward side and of 25 ppb (2.5%) on the windward side. Cumulative traffic emissions produce very high PS mixing-ratios in the lower part of the canyon ($0 < z/l_0 < 1.0$). The concentration of PS decreases smoothly with height on the leeward side but sharply varies on the windward side, e.g., concentrations are higher on the windward side when $0 < z/l_0 < 1.0$ but on the leeward side when $1.0 < z/l_0 < 2.0$. This indicates noticeable segregation between the lower and upper compartments of the deep street canyon due to the presence of two counter-rotating vortices that are captured by the LES and multi-box models. The upper vortex is driven by the ambient wind in the shear layer at the rooftop ($z/l_0 = 2.0$) so that the characteristics of the vertical profiles are similar to those of the regular canyon, while the lower vortex is driven by the upper vortex at approximately $z/l_0 = 1.0$ (or slightly lower) (Eliasson et al., 2006; Zhong et al., 2015).

Considering the chemically reactive species, NO concentrations are slightly underestimated on both sides of the canyon as for the regular canyon, with the maximum difference of 74.9 ppb (9.5%) in $Box_{[1,4]}$ on the windward corner. NO_2 is overestimated by the 32-box model, especially for the windward side (~6%). The O_3 concentrations are slightly underestimated by the 32-box model in the upper vortex on the windward side (~5%), and then are overestimated when air parcel moves to the upper leeward side and to the lower vortex (~10%). Although HO_x concentrations are still higher in the 32-box model compared to the LES, the spatial profiles of HO_2 are well reproduced due to a longer diffusion time in the deep canyon in contrast to the regular canyon. Errors in modelled concentrations (solid and dash lines with the same color) always become larger at $0 < z/l_0 < 1.0$ but become closer at $1.0 < z/l_0 < 2.0$. For example, the 32-box model overestimates NO_2 and O_3 by 14.9% and 27.4% on the leeward side, and by 18.1% and 23.1% on the windward side at the street level ($0 < z/l_0 < 0.25$), but those differences decrease to 8.1%, 17.8%, 14.4% and -10.0% at the rooftop level ($0.75 < z/l_0 < 1.0$), respectively. Therefore, when applying the grid assumption to simulate reactive species in street canyons, it is necessary to consider the inherent uncertainty due to chemical reactions being too fast in particular at the street level, which may lead to an overestimation of pedestrian exposure risks.

3.3. The model performance with the simple NO_x-O_3 cycle

The performance of the multi-box models has been further evaluated with the simplified NO_x-O_3 chemical reactions:

$$NO + O_3 \rightarrow NO_2 \tag{23}$$

$$NO_2 + h\nu \xrightarrow{O_2} NO + O_3 \tag{24}$$

where *hv* represents solar photons. The production and photodegradation coefficients of NO_2 are taken from the RCS chemistry, which are 4.01×10^{-4} ppb^{-1} s^{-1} and 9.20×10^{-3} s^{-1}, respectively. The QSSA is adopted for the calculation. The computation time for the multi-box model using the simple NO_x-O_3 cycle is much quicker (~40 s) than that using RCS chemistry. Table 4 illustrates the time- and spatial-averaged mixing-ratios of NO, NO_2, O_3, NO_x, O_x and NO_2/NO ratios with solely NO_x-O_3 reactions during the final hour in the regular and deep canyons. The modelled NO_x concentrations of the LES model are about 1.9% lower in the regular canyon but are slightly higher in the deep canyon compared to the box models, partly because of strong turbulent fluctuations in the LES. As expected, NO_2 concentrations gradually reduce by 10-13% in the regular canyon without involving OH/HO_2 chemicals, thereby decreasing O_x contents to a similar magnitude. This reduction is rather significant (37-41%) in the deep canyon, resulting in dramatically lower NO_2/NO ratios, which is demonstrated by Zhong et al. (2017). In comparison with the LES outputs, O_3 concentrations are underestimated by the box models to different extents in both regular and deep canyons, which differs from its trends of overestimation with the RCS chemistry. Overall the multi-box models performed better than the one-box and two-box models in simulating all reactive species except O_3.

Modelling differences between the four models shrink when using the very simplified chemical reactions in contrast to the NO_x-O_3-VOC chemical scheme. More specifically, Fig. 5 presents vertical profiles of the difference of NO, NO_2 and O_3 concentrations under different chemical schemes using the multi-box models and the LES, respectively. It clearly exhibits the direct contributions from the VOCs mechanisms spatially, which, in general, shows more substantial influences on the modelling results of the multi-box model compared to those of the LES. The contributions of VOCs are significantly enhanced in the deep street canyon compared to the regular canyon; involving VOCs tends to have greater impacts on local emitted species such as NO and NO_2 in the lower compartments (i.e., $0 < z/l_0 < 1.0$) and on remote species such as O_3 in the upper compartments (i.e., $1.0 < z/l_0 < 2.0$). Although there are some differences between the performance of the multi-box models and the LES, the multi-box models reproduce well the contribution of VOCs to the vertical distribution of NO_2 and O_3.

Fig. 6 illustrates the vertical distributions of NO, NO_2, and O_3 in the regular (a, b, c) and deep (d, e, f) street canyons (i.e., horizontal-averaged concentration cross $-0.5 < x/l_0 < 0.5$) and along the canyon walls (i.e., $-0.5 < x/l_0 < -0.25$ and $0.25 < x/l_0 < 0.5$). In the regular canyon, NO is well-simulated with negligible difference between two models. The vertical profile of NO_2 is overestimated by the 16-box model due to segregation. Nevertheless, extent of overestimation in NO_2 becomes smaller compared to the simulations with NO_x-O_3-VOC chemistry, leading to relatively lower O_3 concentrations along the leeward wall. However, underestimation of O_3 becomes larger on the windward side, with a maximum difference of 4.8 ppb at the rooftop ($0.75 < z/l_0 < 1.0$). In the deep canyon, we also obtained satisfied vertical distributions of all three species from the 32-box model compared to those in the LES. Concentration gradients of NO_2 and O_3 lessen when applying the simple NO_x-O_3 cycle, especially for the street level. NO_2 is still overestimated on the windward side and underestimated on the leeward side, but to a much acceptable degree compared to the scenario with the RCS (Fig. 4). The trends of O_3 are the same as that of the regular canyon in the upper vortex ($1.0 < z/l_0 < 2.0$), e.g., an underestimation on the windward side and overestimation on the leeward side but are consistent with the LES in the lower vortex ($0 < z/l_0 < 1.0$). This indicates that the modelling domain with VOC emissions (e.g., high coverage of vegetation) should consider using air quality models with resolution as high possible to diminish the segregation effects in chemistry.

4. Conclusions

A process-based multi-box photochemical street-canyon model, with a flexible number of boxes and based on a set of transport parameters calculated from the LES outputs is developed in this study. The performance of this street-scale chemical transport model coupled with NO_x-O_3-VOC chemistry (or a simplified NO_x-O_3 cycle), for modelling reactive species in the regular (AR = 1) and deep (AR = 2) street canyons, is compared to published LES data and to one- and two-box simulations. Results show that the model configured with a single box captures the average state of air pollutants in street canyons, and the results are consistent with previous studies (Bright et al., 2013; Zhong et al., 2016). Compared with the benchmark LES simulation, the multi-box model reproduces well the spatial contrast in pollutant concentrations inside the street canyons in particular with a chemically inert passive scalar. Namely, the spatial concentration patterns have been captured for the regular street canyon (i.e., single primary vortex), as well as for the deep street canyon (i.e., two counter-rotating vortices). For the regular canyon, it is found that the NO and O_3 titration reaction becomes more effective due to less segregation along the windward facet, leading to an underestimate of O_3 and an overestimate of NO_2 levels. On the leeward side, the overestimated NO_2 results in an overestimation of O_3 through photolysis. An additional overestimation of NO_2 is attributed to OH/HO_2 chemistry. The impact of segregation effects on the reactive species is substantial, in particular for short-lived species. The OH and HO_2 concentrations are overestimated by the multi-box model, their vertical variations are not very significant compared to the LES because of their very short chemical timescales.

In a deep canyon with poor ventilation, the relationship of reactive species in the upper compartment between the 32-box and LES models is consistent with those in the regular canyon. However, in the lower compartments of the canyon, O_3 is always overestimated, and there are obvious variations of OH and HO_2 concentrations along the vertical direction. Additionally, under the simple NO_x-O_3 cycle, the differences between the multi-box model and the LES become smaller particularly for the deep canyon. Although the effects of VOC chemistry on reactive species such as NO_2 are underestimated compared to the LES, the multi-box models capture the vertical contribution of VOCs to these pollutants in street canyons, and are a significant step forward from the simple one- and two-box models. The multi-box model is less computationally efficient than the typical one-box (~1 s) and two-box models (~8 s), but it can offer spatial information on reactive species within street canyons based on coupled chemical-transport processes (with VOC chemistry) in a fairly short computational times (~6 min) compared to the LES (e.g., ~10 days in Zhong et al. (2017)). Overall, the multi-box model enables insightful investigations into the multiple processes as well as their complex interactions and is of practical utility for air quality assessment or pollution mitigation management in street canyons.

Further works may focus on adopting the multi-box model to simulate air pollution in street canyons with spatially segregated emissions due to the presence of vegetation. More detailed chemical schemes (e.g., Master Chemical Mechanism, MCM*v*3.0 (Saunders et al., 2003)) can be incorporated into the model. The evaluation of modelling results with field measurements is recommended. A more challenging task is to merge the effects of airflow parallel to the street axis on the diffusion and transformation of chemical species, which would enable for a wider range of model applications.

Acknowledgements

The authors thanks Dr Vivien Bright for provision of the reduced chemical scheme (RCS). YD would like to thank the University of Birmingham's BlueBEAR HPC service (http://www.bear.bham.ac.uk) for providing the computational resource. ARMK acknowledges funding support of the Natural Environment Research Council (grants NE/S013814/1, NE/S003487/1). The comments of the anonymous reviewers are gratefully acknowledged.

References

Abhijith, K., Kumar, P., Gallagher, J., McNabola, A., Baldauf, R., Pilla, F., Broderick, B., Di Sabatino, S., Pulvirenti, B., 2017. Air pollution abatement performances of green infrastructure in open road and built-up street canyon environments–A review. Atmospheric Environment 162 71-86.

Ahmad, K., Khare, M., Chaudhry, K., 2005. Wind tunnel simulation studies on dispersion at urban street canyons and intersections—a review. Journal of Wind Engineering and Industrial Aerodynamics 93(9) 697-717.

Alexandrov, V., Sameh, A., Siddique, Y., Zlatev, Z., 1997. Numerical integration of chemical ODE problems arising in air pollution models. Environmental Modeling & Assessment 2(4) 365-377.

Baik, J.-J., Kang, Y.-S., Kim, J.-J., 2007. Modeling reactive pollutant dispersion in an urban street canyon. Atmospheric Environment 41(5) 934-949.

Baker, J., Walker, H.L., Cai, X., 2004. A study of the dispersion and transport of reactive pollutants in and above street canyons—a large eddy simulation. Atmospheric Environment 38(39) 6883-6892.

Boulter, P., Barlow, T., Latham, S., McCrae, I., 2009. Emission factors 2009: Report 1-a review of methods for determining hotexhaust emission factors for road vehicles. TRL Published Project Report.

Bright, V.B., Bloss, W.J., Cai, X., 2013. Urban street canyons: Coupling dynamics, chemistry and within-canyon chemical processing of emissions. Atmospheric Environment 68 127-142.

Cai, X.-M., Barlow, J., Belcher, S., 2008. Dispersion and transfer of passive scalars in and above street canyons—large-eddy simulations. Atmospheric Environment 42(23) 5885-5895.

Cai, X., 2012. Effects of differential wall heating in street canyons on dispersion and ventilation characteristics of a passive scalar. Atmospheric Environment 51 268-277.

Chew, L.W., Aliabadi, A.A., Norford, L.K., 2018. Flows across high aspect ratio street canyons: Reynolds number independence revisited. Environmental Fluid Mechanics 18(5) 1275-1291.

Cui, Z., Cai, X., J. Baker, C., 2004. Large‐eddy simulation of turbulent flow in a street canyon. Quarterly Journal of the Royal Meteorological Society 130(599) 1373-1394.

Driscoll, J.F., Chen, R.-H., Yoon, Y., 1992. Nitric oxide levels of turbulent jet diffusion flames: effects of residence time and Damkohler number. Combustion and Flame 88(1) 37-49.

Eliasson, I., Offerle, B., Grimmond, C., Lindqvist, S., 2006. Wind fields and turbulence statistics in an urban street canyon. Atmospheric Environment 40(1) 1-16.

Fellini, S., Ridolfi, L., Salizzoni, P., 2020. Street canyon ventilation: Combined effect of cross‐section geometry and wall heating. Quarterly Journal of the Royal Meteorological Society 146(730) 2347-2367.

Garmory, A., Kim, I., Britter, R., Mastorakos, E., 2009. Simulations of the dispersion of reactive pollutants in a street canyon, considering different chemical mechanisms and micromixing. Atmospheric Environment 43(31) 4670-4680.

Garmory, A., Richardson, E., Mastorakos, E., 2006. Micromixing effects in a reacting plume by the stochastic fields method. Atmospheric Environment 40(6) 1078-1091.

Gelbard, F., Seinfeld, J.H., 1980. Simulation of multicomponent aerosol dynamics. Journal of colloid and Interface Science 78(2) 485-501.

Gromke, C., Buccolieri, R., Di Sabatino, S., Ruck, B., 2008. Dispersion study in a street canyon with tree planting by means of wind tunnel and numerical investigations–evaluation of CFD data with experimental data. Atmospheric Environment 42(37) 8640-8650.

Gromke, C., Ruck, B., 2007. Influence of trees on the dispersion of pollutants in an urban street canyon—experimental investigation of the flow and concentration field. Atmospheric Environment 41(16) 3287-3302.

Heard, D.E., Pilling, M.J., 2003. Measurement of OH and HO_2 in the troposphere. Chemical Reviews 103(12) 5163-5198.

Jacobson, M.Z., Jacobson, M.Z., 2005. Fundamentals of atmospheric modeling. Cambridge university press.

Jacobson, M.Z., Seinfeld, J.H., 2004. Evolution of nanoparticle size and mixing state near the point of emission. Atmospheric Environment 38(13) 1839-1850.

Jacobson, M.Z., Tabazadeh, A., Turco, R.P., 1996. Simulating equilibrium within aerosols and nonequilibrium between gases and aerosols. Journal of Geophysical Research: Atmospheres 101(D4) 9079-9091.

Jasak, H., Jemcov, A., Tukovic, Z., 2007. OpenFOAM: A C++ library for complex physics simulations, International workshop on coupled methods in numerical dynamics. IUC Dubrovnik Croatia, pp. 1-20.

Kim, M.J., Park, R.J., Kim, J.-J., 2012. Urban air quality modeling with full O3–NOx–VOC chemistry: Implications for O3 and PM air quality in a street canyon. Atmospheric Environment 47 330-340.

Kovar-Panskus, A., Louka, P., Sini, J.-F., Savory, E., Czech, M., Abdelqari, A., Mestayer, P., Toy, N., 2002. Influence of geometry on the mean flow within urban street canyons–a comparison of wind tunnel experiments and numerical simulations. Water, air and soil pollution: focus 2(5) 365-380.

Krol, M.C., Molemaker, M.J., de Arellano, J.V.G., 2000. Effects of turbulence and heterogeneous emissions on photochemically active species in the convective boundary layer. Journal of Geophysical Research: Atmospheres 105(D5) 6871-6884.

Kukkonen, J., Olsson, T., Schultz, D., Baklanov, A., Klein, T., Miranda, A., Monteiro, A., Hirtl, M., Tarvainen, V., Boy, M., 2012. A review of operational, regional-scale, chemical weather forecasting models in Europe. Atmospheric Chemistry and Physics 12(1) 1-87.

Kwak, K.-H., Baik, J.-J., 2012. A CFD modeling study of the impacts of NOx and VOC emissions on reactive pollutant dispersion in and above a street canyon. Atmospheric Environment 46 71-80.

Lee, J.D., Lewis, A.C., Monks, P.S., Jacob, M., Hamilton, J.F., Hopkins, J.R., Watson, N.M., Saxton, J.E., Ennis, C., Carpenter, L.J., 2006. Ozone photochemistry and elevated isoprene during the UK heatwave of August 2003. Atmospheric Environment 40(39) 7598-7613.

Li, X.-X., Leung, D.Y., Liu, C.-H., Lam, K.M., 2008. Physical modeling of flow field inside urban street canyons. Journal of Applied Meteorology and Climatology 47(7) 2058-2067.

Lietzke, B., Vogt, R., 2013. Variability of CO_2 concentrations and fluxes in and above an urban street canyon. Atmospheric Environment 74 60-72.

Liu, C.-H., Leung, D.Y., 2008. Numerical study on the ozone formation inside street canyons using a chemistry box model. Journal of Environmental Sciences 20(7) 832-837.

Murena, F., 2012. Monitoring and modelling carbon monoxide concentrations in a deep street canyon: application of a two-box model. Atmospheric pollution research 3(3) 311-316.

Murena, F., Favale, G., Vardoulakis, S., Solazzo, E., 2009. Modelling dispersion of traffic pollution in a deep street canyon: Application of CFD and operational models. Atmospheric Environment 43(14) 2303-2311.

Nikolova, I., MacKenzie, A.R., Cai, X., Alam, M.S., Harrison, R.M., 2016. Modelling component evaporation and composition change of traffic-induced ultrafine particles during travel from street canyon to urban background. Faraday discussions 189 529-546.

Oke, T.R., 1988. Street design and urban canopy layer climate. Energy and buildings 11(1-3) 103-113.

R Core Team, T., 2019. R: A language and environment for statistical computing. Vienna, Austria.

Salizzoni, P., Soulhac, L., Mejean, P., 2009. Street canyon ventilation and atmospheric turbulence. Atmospheric Environment 43(32) 5056-5067.

Saunders, S.M., Jenkin, M.E., Derwent, R., Pilling, M., 2003. Protocol for the development of the Master Chemical Mechanism, MCM v3 (Part A): tropospheric degradation of non-aromatic volatile organic compounds. Atmospheric Chemistry and Physics 3(1) 161-180.

Schlichting, H., Gersten, K., 2016. Boundary-layer theory. Springer.

Takano, Y., Moonen, P., 2013. On the influence of roof shape on flow and dispersion in an urban street canyon. Journal of Wind Engineering and Industrial Aerodynamics 123 107-120.

Vardoulakis, S., Fisher, B.E., Pericleous, K., Gonzalez-Flesca, N., 2003. Modelling air quality in street canyons: a review. Atmospheric Environment 37(2) 155-182.

Watson, L., Shallcross, D., Utembe, S., Jenkin, M., 2008. A Common Representative Intermediates (CRI) mechanism for VOC degradation. Part 2: Gas phase mechanism reduction. Atmospheric Environment 42(31) 7196-7204.

Wu, L., Hang, J., Wang, X., Shao, M., Gong, C., 2021. APFoam 1.0: integrated computational fluid dynamics simulation of O 3–NO x–volatile organic compound chemistry and pollutant dispersion in a typical street canyon. Geoscientific Model Development 14(7) 4655-4681.

Yang, H., Chen, T., Lin, Y., Buccolieri, R., Mattsson, M., Zhang, M., Hang, J., Wang, Q., 2020. Integrated impacts of tree planting and street aspect ratios on CO dispersion and personal exposure in full-scale street canyons. Building and Environment 169 106529.

Yang, H., Lam, C.K.C., Lin, Y., Chen, L., Mattsson, M., Sandberg, M., Hayati, A., Claesson, L., Hang, J., 2021. Numerical investigations of Re-independence and influence of wall heating on flow characteristics and ventilation in full-scale 2D street canyons. Building and Environment 189 107510.

Zhang, K., Chen, G., Zhang, Y., Liu, S., Wang, X., Wang, B., Hang, J., 2020. Integrated impacts of turbulent mixing and NOX-O3 photochemistry on reactive pollutant dispersion and intake fraction in shallow and deep street canyons. Science of the Total Environment 712 135553.

Zhong, J., Cai, X.-M., Bloss, W.J., 2015. Modelling the dispersion and transport of reactive pollutants in a deep urban street canyon: Using large-eddy simulation. Environmental Pollution 200 42-52.

Zhong, J., Cai, X.-M., Bloss, W.J., 2016. Modelling photochemical pollutants in a deep urban street canyon: application of a coupled two-box model approximation. Atmospheric Environment 143 86-107.

Zhong, J., Cai, X.-M., Bloss, W.J., 2017. Large eddy simulation of reactive pollutants in a deep urban street canyon: Coupling dynamics with O_3-NO_x-VOC chemistry. Environmental Pollution 224 171-184.

Zhong, J., Nikolova, I., Cai, X., MacKenzie, A.R., Alam, M.S., Xu, R., Singh, A., Harrison, R.M., 2020a. Neighbourhood-scale dispersion of traffic-induced ultrafine particles in central London: WRF large eddy simulations. Environmental Pollution 266 115223.

Zhong, J., Nikolova, I., Cai, X., MacKenzie, A.R., Alam, M.S., Xu, R., Singh, A., Harrison, R.M., 2020b. Traffic-induced multicomponent ultrafine particle microphysics in the WRF v3. 6.1 large eddy simulation model: General behaviour from idealised scenarios at the neighbourhood-scale. Atmospheric Environment 223 117213.

Zhong, J., Nikolova, I., Cai, X., MacKenzie, A.R., Harrison, R.M., 2018. Modelling traffic-induced multicomponent ultrafine particles in urban street canyon compartments: Factors that inhibit mixing. Environmental Pollution 238 186-195.

Figures

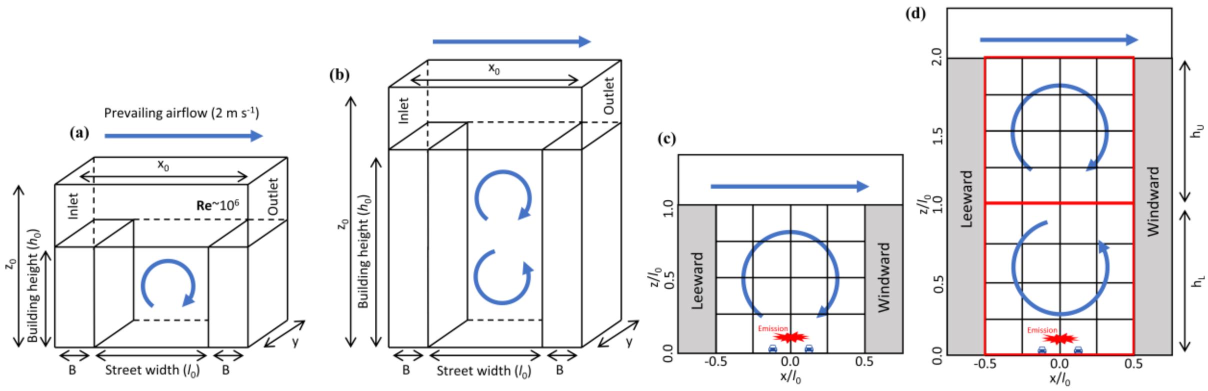

Fig. 1. Schematic diagram of (a) the LES domain for a regular urban street canyon where x_0 = 24 m, y_0 = 40 m and z_0 = 90 m, and canyon geometries l_0 = h_0 = 18 m, wall width B = 3 m, modified from Bright et al. (2013); (b) the LES domain for a deep canyon x_0 = 36 m, y_0 = 40 m and z_0 = 112 m, and canyon geometries l_0 = 18 m, h_0 = 36 m and B = 9 m, modified from Zhong et al. (2015); (c) the equivalent multi-box (16) model for the regular canyon; (d) the two-box model denoted by the red frame, where the height of upper (h_U) and lower compartments (h_L) is 9 m, and the multi-box (32) model for the deep canyon. See text for details.

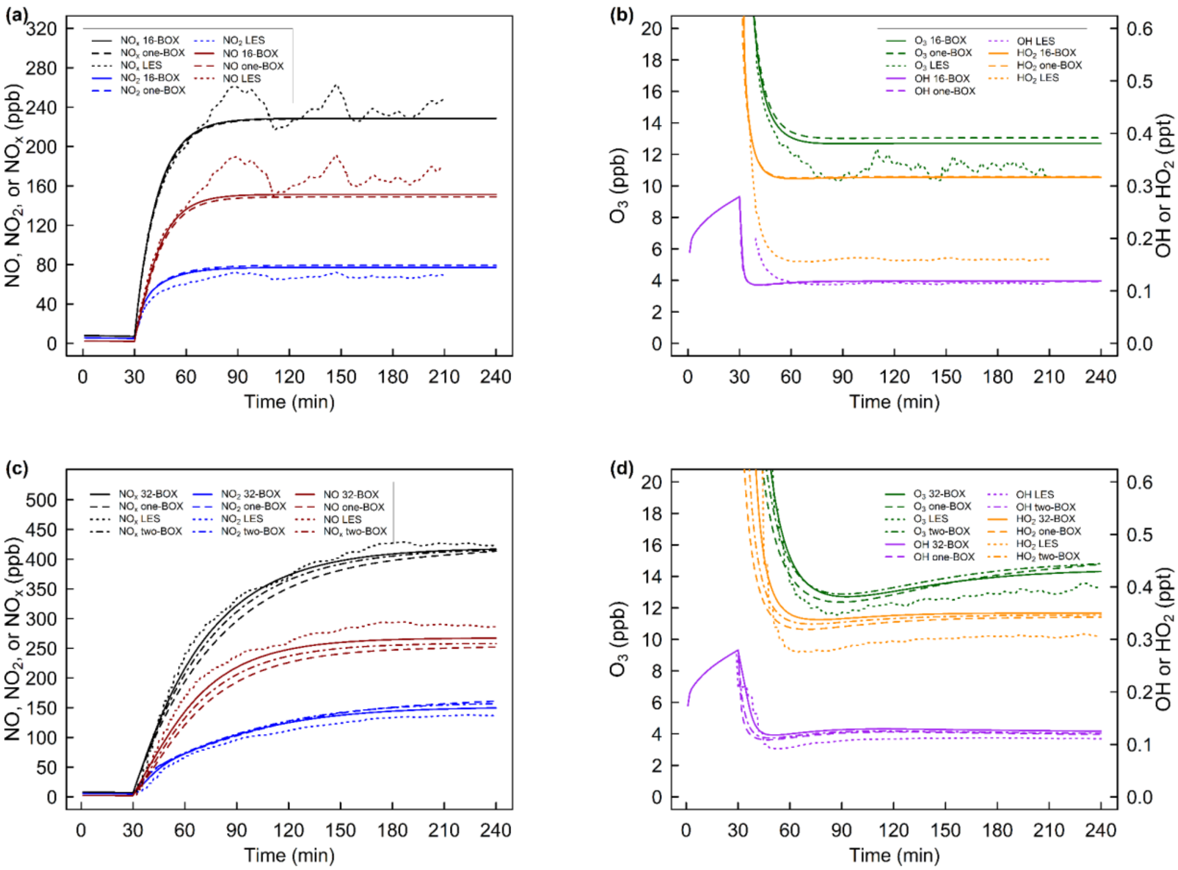

Fig. 2. Temporal variation of the spatially averaged mixing-ratio of NO, NO_2, NO_x, O_3 (ppb), OH and HO_2 (ppt) calculated using the LES, multi-box and a typical one-box models for the regular (a, b) and deep (c, d) street canyons. Two-box simulations are conducted only in the deep canyon, see text for details.

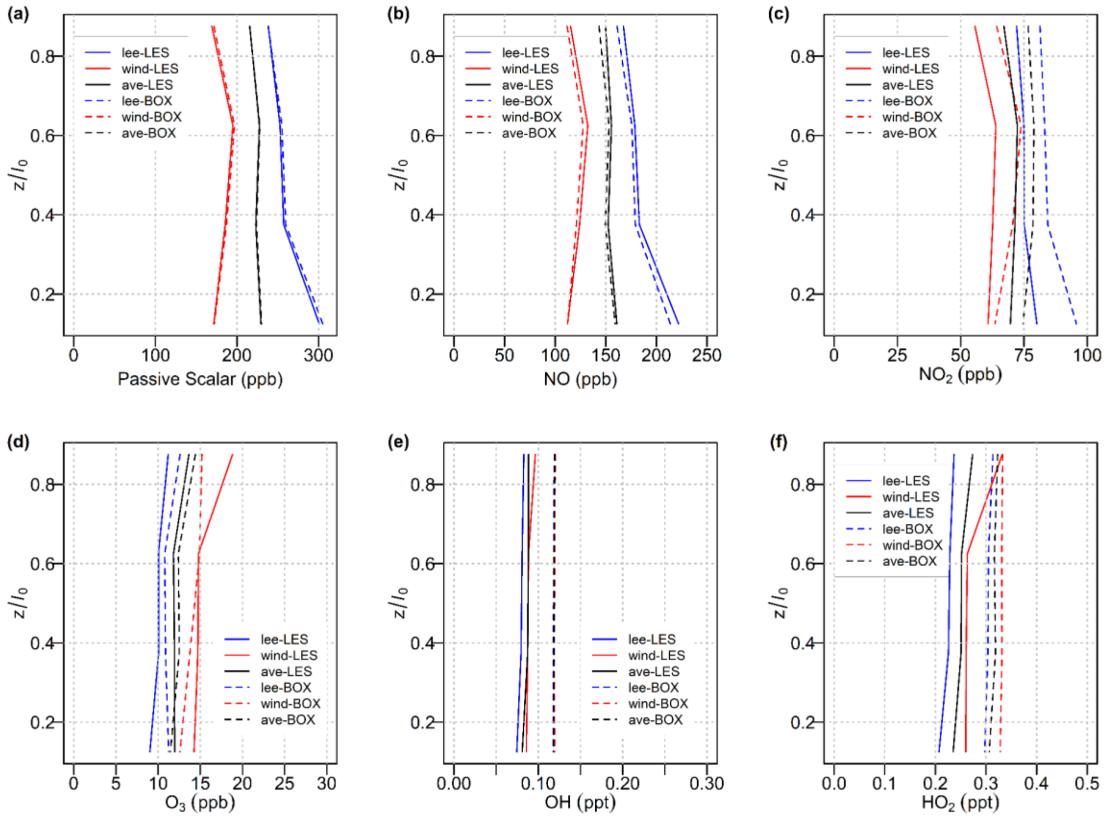

Fig. 3. Vertical profiles of the time-averaged mixing-ratios of PS, NO, NO_2, O_3, OH and HO_2 in the regular street canyon ($-0.5 < x/l_0 < 0.5$) represented by the black lines, along with the leeward wall ($-0.5 < x/l_0 < -0.25$) represented the by blue lines, and along with the windward wall ($0.25 < x/l_0 < 0.5$) represented by the red lines. Solid and dash lines indicate modelling results from LES and multi-box models, respectively.

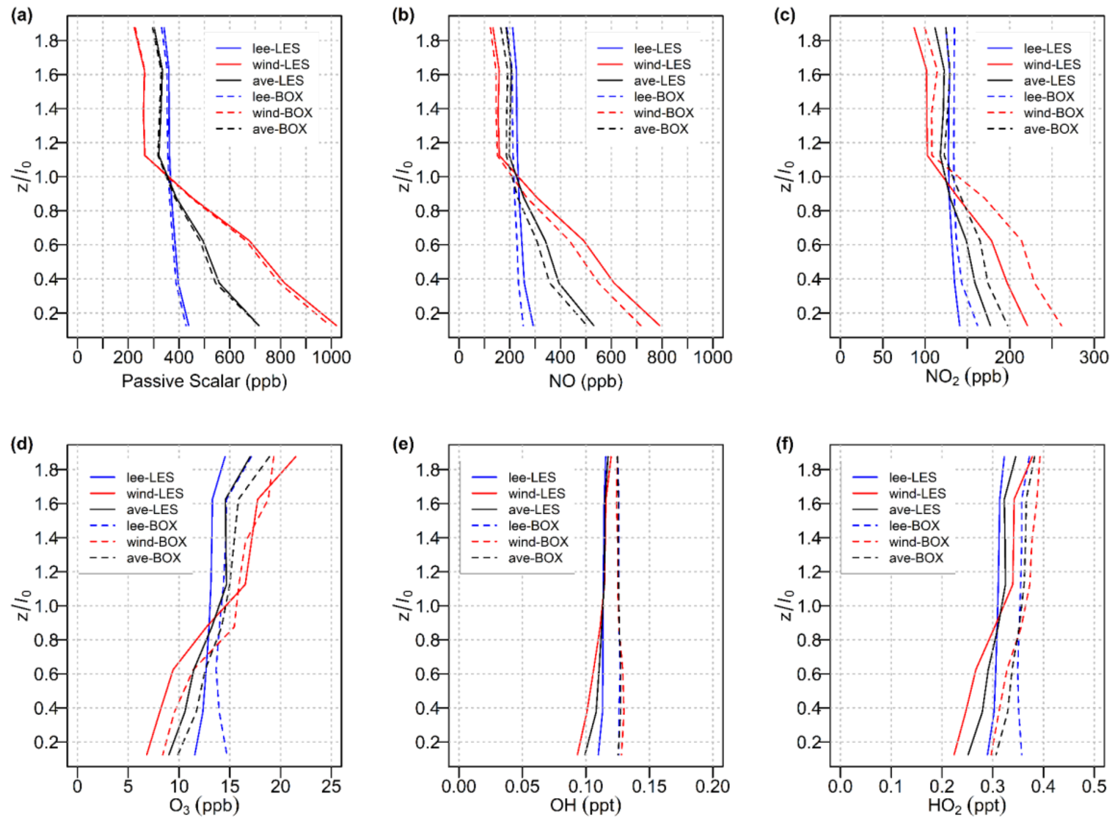

Fig. 4. Vertical profiles of the time-averaged mixing-ratios of PS, NO, NO_2, O_3, OH and HO_2 in the deep street canyon ($-0.5 < x/l_0 < 0.5$) represented by the black lines, along with the leeward wall ($-0.5 < x/l_0 < -0.25$) represented the by blue lines, and along with the windward wall ($0.25 < x/l_0 < 0.5$) represented by the red lines. Solid and dash lines indicate modelling results from LES and multi-box models, respectively.

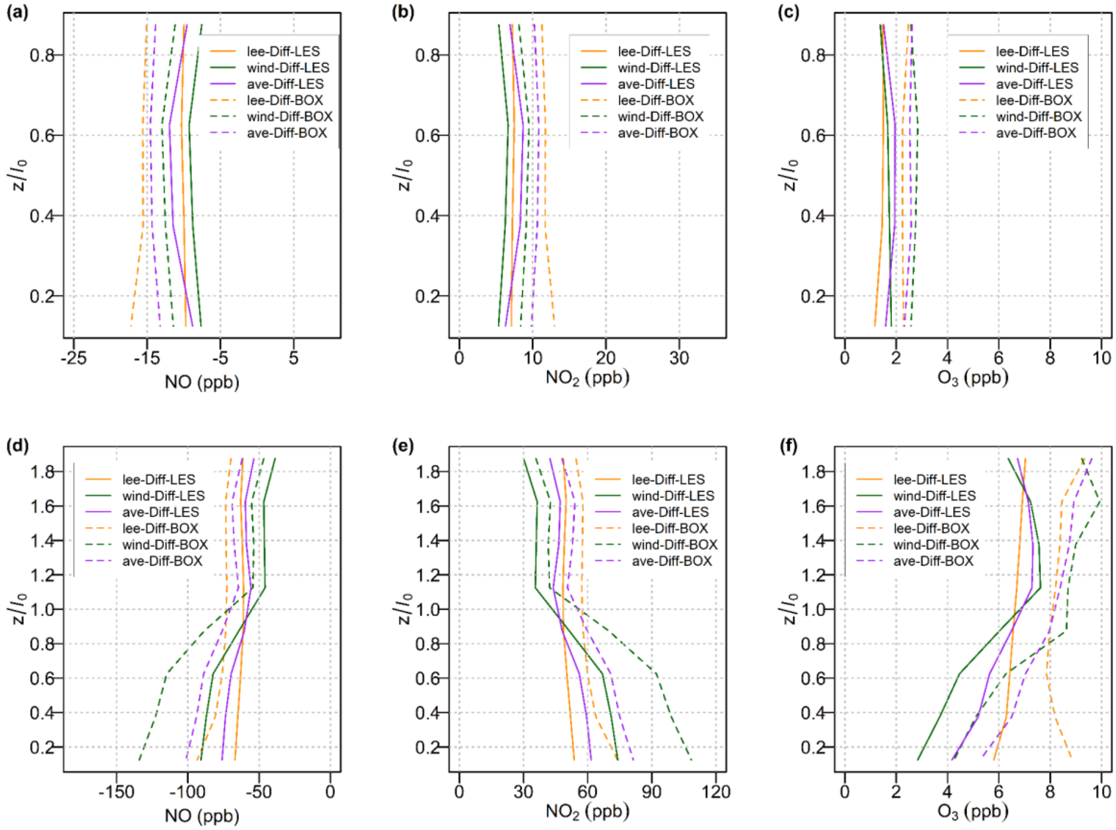

Fig. 5. Vertical profiles of the difference of NO, NO_2 and O_3 concentrations under different chemical schemes (modelling results with the VOC chemistry minus results with the simple NO_x-O_3 chemistry) in regular (a, b, c) and deep (d, e, f) street canyons ($-0.5 < x/l_0 < 0.5$) represented by the purple lines, along with the leeward wall ($-0.5 < x/l_0 < -0.25$) represented the by orange lines, and along with the windward wall ($0.25 < x/l_0 < 0.5$) represented by the green lines. Solid and dash lines indicate modelling results from LES and multi-box models, respectively.

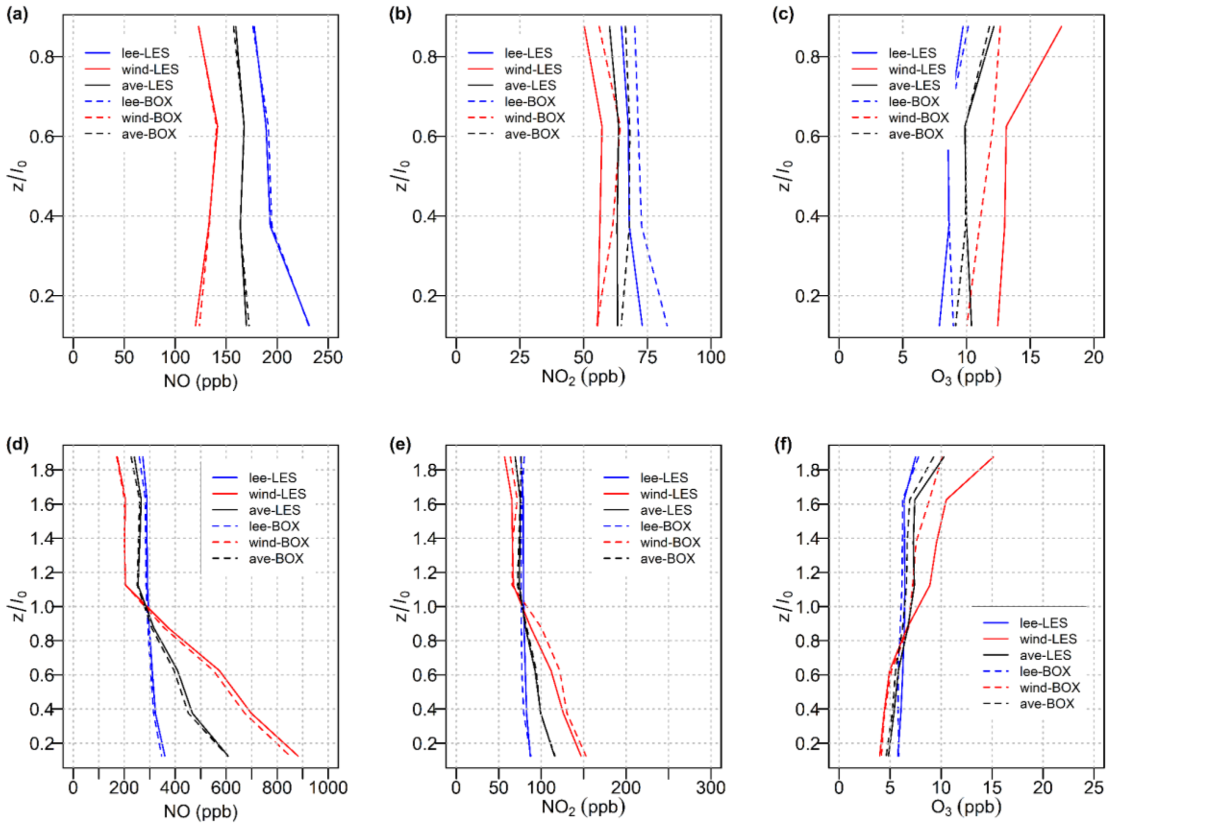

Fig. 6. Vertical profiles of the time-averaged mixing-ratios of NO, NO_2, and O_3 in regular (a, b, c) and deep (d, e, f) street canyons ($-0.5 < x/l_0 < 0.5$) represented by the black lines, along with the leeward wall ($-0.5 < x/l_0 < -0.25$) represented the by blue lines, and along with the windward wall ($0.25 < x/l_0 < 0.5$) represented by the red lines. Solid and dash lines indicate modelling results from LES and multi-box models, respectively.

Tables

Table 1. Time-averaged mixing-ratios from LES, the multi (16/32)-box model, and the one-box and two-box models with RCS chemistry for urban street canyons.

		Mixing-ratio (ppb)									
		(a) LES	(b) 16/32-box	(c) Two-box	(d) One-box	(b) - (a)	(c) - (a)	(d) - (a)	[(b)-(a)]/(a) (%)	[(c)-(a)]/(a) (%)	[(d)-(a)]/(a) (%)
The regular street canyon (AR = 1)	PS	223.86	224.33	-	223.85	0.47	-	-0.01	0.21	-	-0.004
	NO	154.66	151.28	-	148.87	-3.38	-	-5.79	-2.19	-	-3.74
	NO_2	70.12	77.19	-	79.35	7.07	-	9.23	10.08	-	13.16
	O_3	12.35	12.70	-	13.05	0.35	-	0.70	2.83	-	5.67
	OH^*	0.086	0.119	-	0.118	0.033	-	0.032	38.37	-	37.21
	HO_2^*	0.253	0.316	-	0.318	0.063	-	0.065	24.90	-	25.69
	NO_x	224.78	228.47	-	228.22	3.69	-	3.44	1.64	-	1.51
	O_x	82.47	89.89	-	92.4	7.42	-	9.93	9.00	-	11.05
	NO_2/NO	0.45	0.51	-	0.53						
The deep street canyon (AR = 2)	PS	430.23	423.53	421.53	417.06	-6.7	-8.7	-13.17	-1.56	-2.02	-3.06
	NO	289.10	266.48	257.48	250.11	-22.62	-31.62	-38.99	-7.82	-10.94	-13.49
	NO_2	136.07	147.84	154.57	156.52	11.77	18.5	20.45	8.65	13.60	15.03
	O_3	13.14	14.19	14.62	14.46	1.05	1.48	1.32	7.99	11.26	10.05
	OH^*	0.11	0.13	0.12	0.12	0.02	0.01	0.01	18.18	9.09	9.09
	HO_2^*	0.31	0.35	0.34	0.34	0.04	0.03	0.03	12.90	9.68	9.68
	NO_x	425.17	414.32	412.05	406.63	-10.85	-13.12	-18.54	-2.55	-3.09	-4.47
	O_x	149.21	162.03	169.19	170.98	12.82	19.98	21.77	8.59	13.39	13.44
	NO_2/NO	0.47	0.55	0.60	0.63						

* Mixing-ratio of OH and HO_2 are presented in part per trillion (ppt).

Table 2. Time-averaged mixing-ratios from LES, the 32-box model and the two-box model with RCS chemistry in the deep canyon.

		Mixing-ratio (ppb)					[(b)-(a)]/(a) (%)	[(c)-(a)]/(a) (%)
		(a) LES	(b) 32-box	(c) Two-box	(b) - (a)	(c) - (a)		
The upper compartment	PS	321.23	315.93	313.65	-5.30	-7.58	-1.65	-2.36
	NO	198.14	182.87	178.03	-15.27	-20.11	-7.71	-10.15
	NO_2	118.44	125.78	129.02	7.34	10.58	6.20	8.93
	O_3	15.21	16.29	16.96	1.08	1.75	7.10	11.51
	OH^*	0.11	0.12	0.12	0.01	0.01	9.09	9.09
	HO_2^*	0.33	0.36	0.37	0.03	0.04	9.09	12.12
	NO_x	316.58	308.65	307.05	-7.93	-9.53	-2.50	-3.01
	O_x	133.65	142.06	145.97	8.41	12.32	6.29	9.22
	NO_2/NO	0.60	0.68	0.72				
The lower compartment	PS	539.23	531.13	529.42	-8.10	-9.81	-1.50	-1.82
	NO	380.06	350.09	336.93	-29.97	-43.13	-7.89	-11.35
	NO_2	153.69	169.90	180.12	16.21	26.43	10.55	17.20
	O_3	11.06	12.09	12.29	1.03	1.23	9.31	11.12
	OH^*	0.11	0.12	0.12	0.01	0.01	9.09	9.09
	HO_2^*	0.28	0.33	0.33	0.05	0.05	17.86	17.86
	NO_x	533.75	519.99	517.05	-13.76	-16.7	-2.58	-3.13
	O_x	164.75	181.99	192.41	17.24	27.66	10.46	16.79
	NO_2/NO	0.40	0.48	0.53				

* Mixing-ratio of OH and HO_2 are presented in part per trillion (ppt).

Table 3. The percentage intensities of segregation between pairs of reactive species from the LES and multi-box models (BOX) for the regular and deep canyons. Bold symbols represent species that directly react with each other in the models, and negative values are shown in red.

		LES					BOX				
		NO	NO_2	O_3	OH	HO_2	NO	NO_2	O_3	OH	HO_2
The regular street canyon (AR = 1)	NO	3.02	-	-	-	-	2.97	-	-	-	-
	NO_2	1.38	0.83	-	-	-	1.61	1.15	-	-	-
	O_3	**-2.79**	-1.64	3.54	-	-	**-1.34**	-0.36	1.61	-	-
	OH	**-0.81**	**-0.27**	**0.76**	0.43	-	**-0.08**	**-0.03**	**0.07**	0.004	-
	HO_2	**-1.43**	**-0.71**	**1.74**	**0.60**	**1.12**	**-0.56**	**-0.20**	**0.42**	**0.02**	**0.15**
The deep street canyon (AR = 2)	NO	26.15	-	-	-	-	26.35	-	-	-	-
	NO_2	10.21	4.18	-	-	-	11.50	5.58	-	-	-
	O_3	**-10.02**	-4.35	5.09	-	-	**-9.35**	-3.86	4.45	-	-
	OH	**-2.75**	**-1.06**	**1.09**	0.31	-	**0.22**	**0.15**	**-0.09**	0.01	-
	HO_2	**-5.13**	**-2.12**	**2.36**	**0.57**	**1.15**	**-3.54**	**-1.45**	**1.56**	**-0.03**	**0.57**

Table 4. Time-averaged mixing-ratios from LES, the multi (16/32)-box model, and the one-box and two-box models with the simple NO_x-O_3 chemistry for urban street canyons.

		Mixing-ratio (ppb)									
		(a) LES	(b) 16/32-box	(c) Two-box	(d) One-box	(b) - (a)	(c) - (a)	(d) - (a)	[(b)-(a)]/(a) (%)	[(c)-(a)]/(a) (%)	[(d)-(a)]/(a) (%)
The regular street canyon (AR = 1)	NO	165.10	165.27	-	163.24	0.17	-	-1.86	0.10	-	-1.13
	NO_2	62.58	66.81	-	68.72	4.22	-	6.14	6.75	-	9.81
	O_3	10.60	10.19	-	10.43	-0.41	-	-0.17	-3.89	-	-1.60
	NO_x	227.69	232.08	-	231.97	4.39	-	4.28	1.93	-	1.88
	O_x	73.18	77.00	-	79.16	3.81	-	5.97	5.21	-	8.16
	NO_2/NO	0.38	0.40	-	0.42						
The deep street canyon (AR = 2)	NO	352.57	344.33	336.85	333.14	-8.24	-15.72	-19.43	-2.34	-4.46	-5.51
	NO_2	85.43	86.30	90.29	92.03	0.87	4.86	6.60	1.02	5.69	7.72
	O_3	6.89	6.38	6.62	6.45	-0.51	-0.27	-0.44	-7.35	-3.95	-6.43
	NO_x	438.00	430.63	427.14	425.17	-7.37	-10.86	-12.83	-1.68	-2.48	-2.93
	O_x	92.32	92.69	96.91	98.48	0.37	4.59	6.15	0.40	4.97	6.67
	NO_2/NO	0.24	0.25	0.27	0.28						